Semipolar ($11\bar{2}2$) and polar (0001) InGaN grown on sapphire substrate by using pulsed metal organic chemical vapor deposition*

Sheng-Rui Xu(许晟瑞)†, Ying Zhao(赵颖), Ren-Yuan Jiang(蒋仁渊), Teng Jiang(姜腾), Ze-Yang Ren(任泽阳), Jin-Cheng Zhang(张进成)‡, and Yue Hao(郝跃)

Key Laboratory of Wide Band-Gap Semiconductor Technology, School of Microelectronics, Xidian University, Xi'an 710071, *China*

(Received 29 September 2016; revised manuscript received 8 November 2016; published online 20 December 2016)

High indium semipolar ($11\bar{2}2$) and polar (0001) InGaN layers each with a thickness of about 100 nm are realized simultaneously on sapphire substrates by pulsed metal organic chemical vapor deposition (MOCVD). The morphology evolution, structural and optical characteristics are also studied. The indium content in the layer of the surface ($11\bar{2}2$) is larger than that of the surface (0001), which is confirmed by reciprocal space map, photoluminescence spectrum and secondary ion mass spectrometer. Additionally, the (0001) surface with island-like morphology shows inhomogeneous indium incorporation, while the ($11\bar{2}2$) surface with a spiral-like morphology shows a better homogeneous In composition. This feature is also demonstrated by the monochromatic cathodoluminescence map.

Keywords: semipolar, GaN, MOCVD

PACS: 78.55.Cr, 81.15.Kk **DOI:** 10.1088/1674-1056/26/2/027801

1. Introduction

Nonpolar and semipolar III–nitrides have been extensively investigated and proven to be a way to be able to effectively improve the characteristics of the light emitting devices (LEDs),[1–3] because the nonpolar and semipolar growth can completely or partially eliminate the polarization-induced internal electric field effect (PE) along the typical polar [0001] *c* direction. The reduction of PE enhances the radiative recombination probability between electron and hole wave-functions and leads to a high internal quantum efficiency, which has experimentally been demonstrated.[4,5] However, there are some reports revealing that the light emitting wavelength of nonpolar *m*-plane laser diodes (LD) was limited to around 500 nm.[6] Consequently, to solve the "green gap" problem, it seems to be a more attractive option using semipolar LEDs to achieve high indium composition.

It should be noted that since the realization of the high-quality green laser diode on the ($20\bar{2}1$) orientation in 2009,[7] a series of semipolar surfaces including {201}, {301}, and {112} has been reported. However, most of these "artificial" semipolar facets such as ($20\bar{2}1$) and (2021) are obtained with the freestanding substrates, namely the homoepitaxy.[8–11] Although the film has low dislocation density ($< 10^6$ cm^{-2}),[12] its practical application is restricted, for the freestanding substrate is extremely expensive in cost and excessively small in size. Compared with the freestanding substrate, the sapphire substrate which is easy to acquire at much lower price will be very promising. Currently, many studies have shown that the ($11\bar{2}2$) plane can be obtained on the *m*-plane sapphire substrate.[13–15] Moreover, the ($11\bar{2}2$) plane is relatively easy to achieve compared with the other semipolar planes.[16]

In this paper, we introduce the pulsed techniques into metal organic chemical vapor deposition (PMOCVD) and realize the high indium incorporation. The growth method in which the reactive atoms are separately supplied to the reactor at different times has been proved to be effective in the InAlN/GaN heterostructure growth reported by our group.[17,18] We achieve the InGaN/GaN/sapphire structure based on such a method and compare the indium incorporated into ($11\bar{2}2$) with that into (0001) plane. The morphology evolution, structural and optical characterization are also discussed.

2. Experimental details

The samples were simultaneously grown on 2-inch (1 inch = 2.54 cm) sapphire (semipolar on *m* plane and polar on *c* plane) substrates by MOCVD through using trimethylgallium (TEGa), trymethylindium (TMIn) and ammonia (NH_3) as precursors and hydrogen as the carrier gas. Prior to growth, all the sapphires were treated with an initial nitridation for the epilayer formation. After this, a low-temperature GaN nucleation layer was grown at 550 °C for 5 min, followed by growing a 0.8-μm thick GaN film at 1000 °C. Then the temperature was reduced to 620 °C for the InGaN layer growth and the detailed growth sequence is shown in Fig. 1. As can be seen,

*Project supported by the National Natural Science Foundation of China (Grant Nos. 61204006 and 61574108) and the Fundamental Research Funds for the Central Universities, China (Grant No. 7214570101).

†Corresponding author. E-mail: shengruixidian@126.com

‡Corresponding author. E-mail: jchzhang@xidian.edu.cn

© 2017 Chinese Physical Society and IOP Publishing Ltd

6-s pulses of TMIn and 3-s pulses of NH_3 were introduced alternately into the MOCVD reactor with the continuous TEGa. The NH_3 pulse always followed the TMIn pulses.

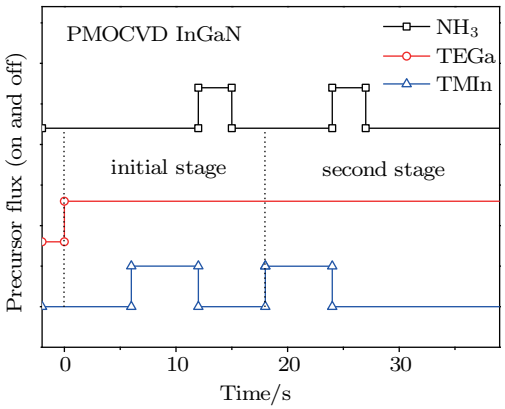


Fig. 1. (color online) Growth sequence of PMOCVD pulses for InGaN barrier layer.

The morphology was characterized by atomic force microscopy (AFM) and scanning electron microscopy (SEM). The indium content was determined by high-resolution x-ray diffraction (HRXRD) and secondary ion mass spectrometer (SIMS). The optical properties were examined by cathodoluminescence (CL) and photoluminescence (PL) spectroscopy.

3. Results and discussion

The surface morphologies of $(11\bar{2}2)$ and (0001) InGaN/GaN assessed by AFM (Agilent 5500) and SEM (Quanta 400 FEG) simultaneously are shown in Fig. 2. With the spiral-like pit morphology in Fig. 2(a) turning into the typical island-like morphology in Fig. 2(c), the root-mean square (RMS) roughness value changes from 11.2 nm to 12.4 nm. Moreover, the pits as shown in Fig. 2(b) with different sizes, arrange along the projection direction of the *c* axis, which is believed to be related to the anisotropic diffusions of atoms on the semipolar surfaces.[19] On the other hand, the formation of the undulated surface morphology is also attributed to the V-shape structure, especially when the film growth contains indium.[20] In contrast, there are a lot of pits on the (0001) plane indicated by the red circles as shown in Fig. 2(d), which are generally considered as an indication of incomplete island coalescence.

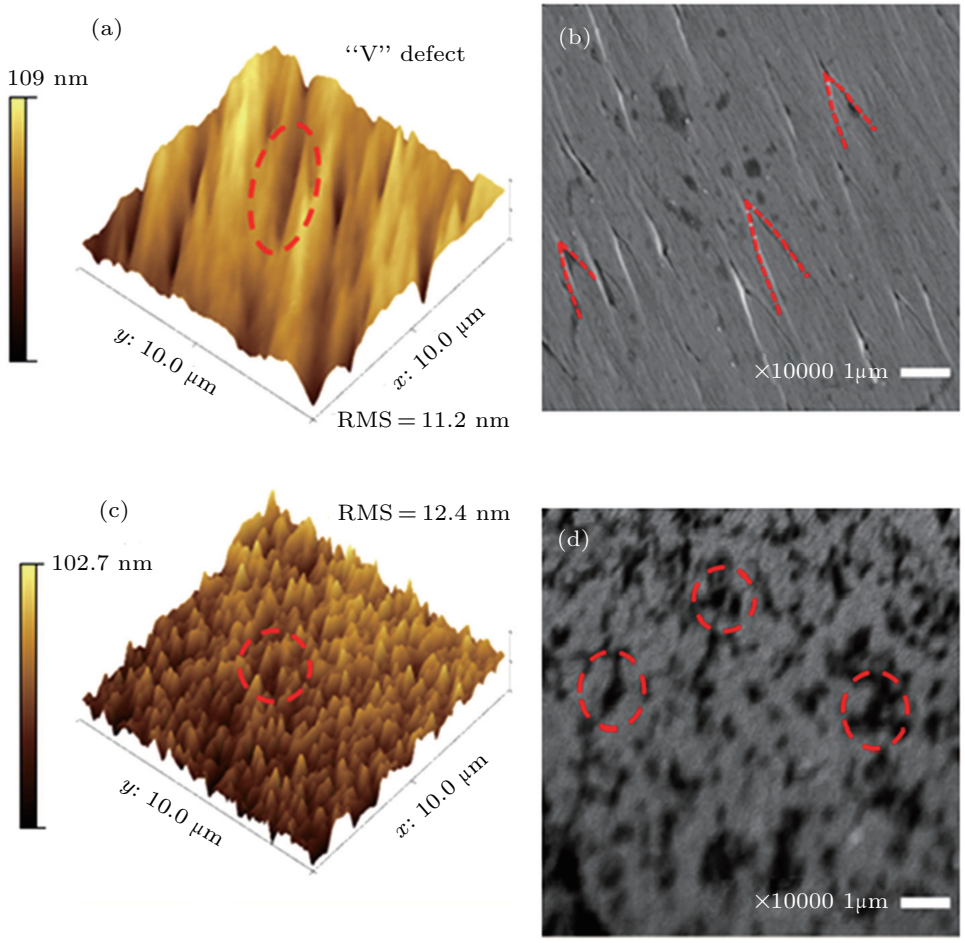


Fig. 2. (color online) The AFM (10 μm×10 μm) and SEM images of the InGaN grown on sapphires with different polarities: $(11\bar{2}2)$ plane [(a) and (b)], (0001) plane [(c) and (d)].

Shown in Figs. 3(a) and 3(b) are the HRXRD (Bruker D8-discover system) results of the symmetrical (002) and asymmetrical (102) reflections of *c*-plane GaN, respectively. The full-width at half-maximum (FWHM) values of the *c*-plane GaN films are

0.17° and 0.22°. The HRXRD (11$\bar{2}$2) FWHM anisotropy with respect to the in-plane beam orientation is also shown in Fig. 3(c). We recorded the on-axis reciprocal space maps (RSMs) along different in-plane directions by HRXRD as shown in Fig. 4.

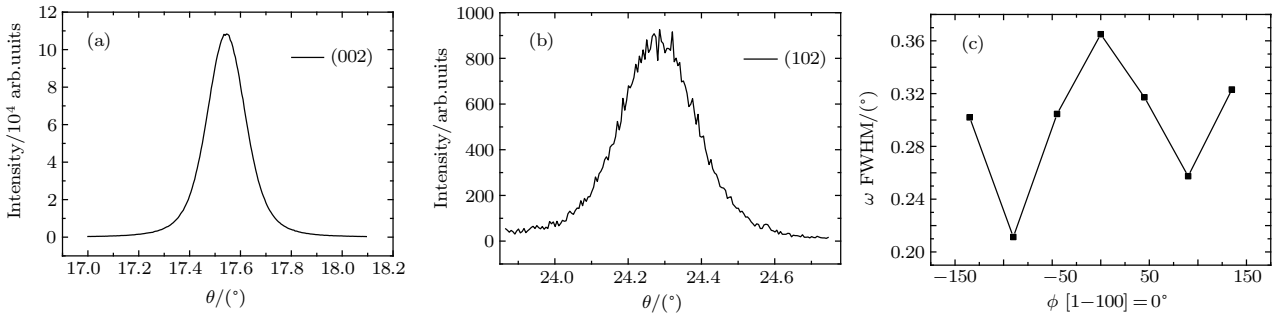


Fig. 3. (a) Symmetric (002) and (b) asymmetric (102) reflection XRD ω-scan rocking curves for c-plane GaN film, (c) XRD (11$\bar{2}$2) FWHM anisotropy with respect to the in-plane beam orientation.

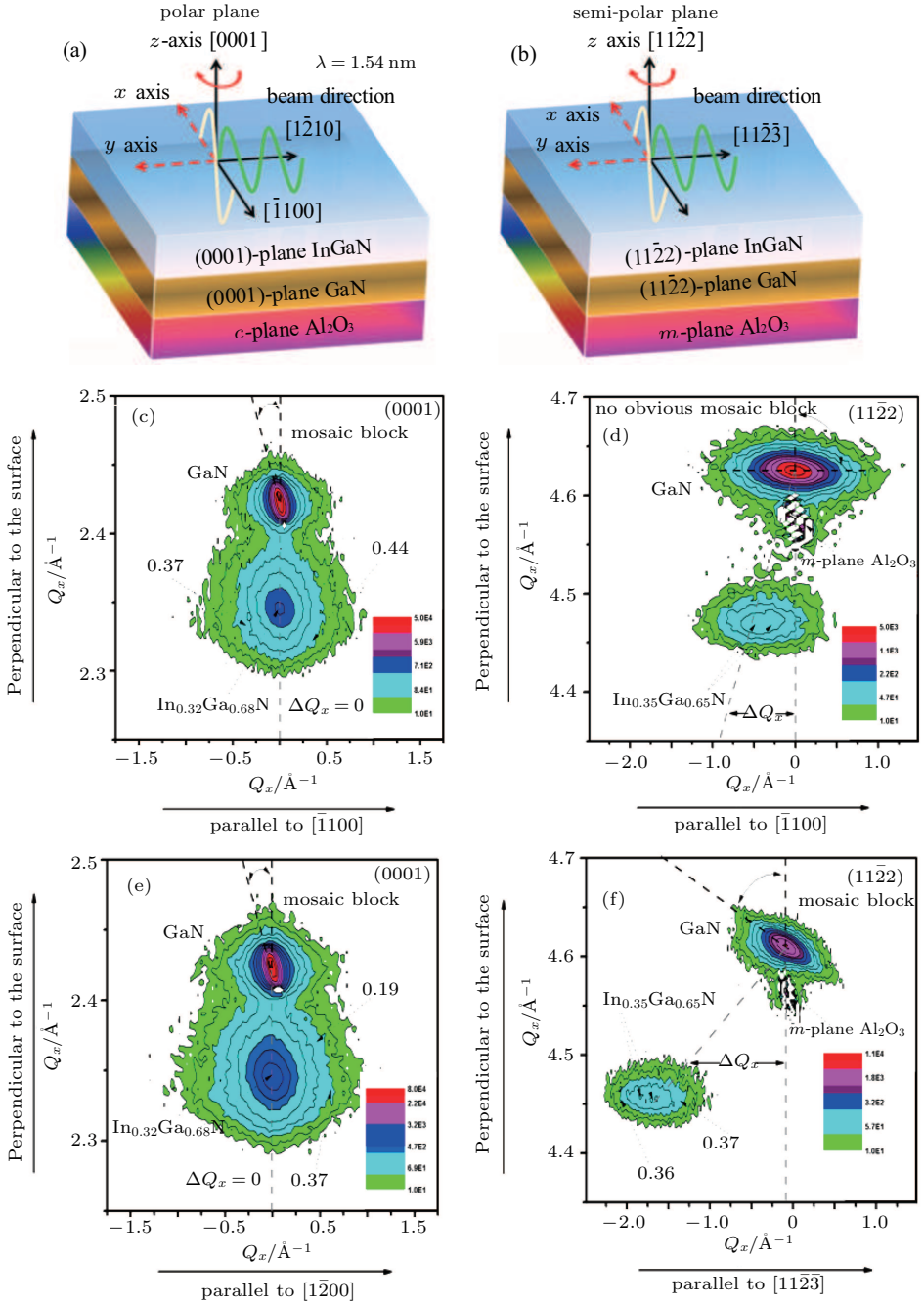


Fig. 4. (color online) Symmetric RSMs for (a) (0001) and (b) (11$\bar{2}$2) InGaN/GaN structures recorded at 90° rotations with respect to each other along both principal, in-plane directions. The x-ray beam is aligned parallelly to (c) [$\bar{1}$100], (e) [1$\bar{2}$10] for polar plane and (d) [1$\bar{1}$00], (f) [11$\bar{2}\bar{3}$] for semipolar plane.

The x-ray incidences are along the well-known *m*-axis [$\bar{1}100$] and *a*-axis [$1\bar{2}10$] direction for the (0001) plane, [$1\bar{1}00$] and [$11\bar{2}\bar{3}$] direction for the ($11\bar{2}\bar{2}$) plane. The in-plane directions are perpendicular to each other in the color map. For the polar surface, no offset in Q_x between InGaN and GaN layer is observed in RSM (Fig. 4(c) and Fig. 4(e)) when the x-ray incidence is along *m* axis nor *a* axis. This indicates that the InGaN layer grew coherently on the GaN film in both directions. However, the result of semipolar surface is distinctly different as shown in Figs. 4(d) and 4(f). Along the [$11\bar{2}\bar{3}$] and [$1\bar{1}00$] direction, the representative InGaN and GaN peaks each show a significant offset in Q_x. Moreover, the offset value along [$11\bar{2}\bar{3}$] is significantly larger than that along [$1\bar{1}00$]. Actually, such an offset in on-axis RSM indicates the glide and bend of threading dislocation in the ($11\bar{2}2$) plane.[21–23] The unequal offset value of the semipolar plane also shows highly anisotropic features compared with that of the polar plane. In addition, we determine the indium content with the help of RSMs as shown in Fig. 4. The indium content is 32% for (0001) plane and 37% for ($11\bar{2}2$) plane, indicating the ($11\bar{2}2$) plane has higher indium incorporation than the (0001) plane. A large indium in-plane fluctuation has been observed in the (0001) plane InGaN.[24] However, the ($11\bar{2}2$) plane presents much better in-plane homogeneity of indium composition. As is well known, the indium content is closely related to growth polarity.[25] It seems that semipolar InGaN can improve the in-plane fluctuations generally existing in polar InGaN layer with the PMOCVD technique.

In order to further confirm that the semipolar surface has more homogeneous indium incorporation, the CL (MonoCL3+) spectrum is depicted in Fig. 5. The SEM images of (0001) and ($11\bar{2}2$) plane are shown in Figs. 5(b) and 5(d), respectively. Correspondingly, figures 5(a) and 5(c) are the monochromatic CL maps taken at 300 K recorded at the energy 2.15 eV. The scan size is 20 μm×20 μm for both samples. A strong contrast of dark area and luminescent spots is observed for (0001) InGaN, whereas a smoother luminous intensity distribution is revealed for ($11\bar{2}2$) InGaN. This suggests that more inhomogeneous indium incorporation into polar InGaN is obtained by PMOCVD.[26]

The optical properties of these two samples are compared by room temperature PL spectra (Jobin Yvon LabRam HR800) as shown in Fig. 6 with a 325-nm He–Cd laser as an excitation source. After normalizing the GaN peak intensity, besides the sharp peak around 3.4 eV associated with GaN, the representative InGaN peaks covering from 500 nm to 650 nm are also detected.[27] Obviously, although the emission intensity of ($11\bar{2}2$) InGaN is lower than that of (0001) InGaN, the wavelength is slightly longer. The PL result further indicates that the semipolar InGaN layer may contain higher indium than the polar InGaN layer. Additionally, a sub-peak at 2.03 eV is observed, demonstrating the existence of indium component unhomogeneity for polar plane InGaN. Furthermore, the blue-violet-band at 2.9 eV is also observed, which is associated with hydrogen–carbon complexes.[28]

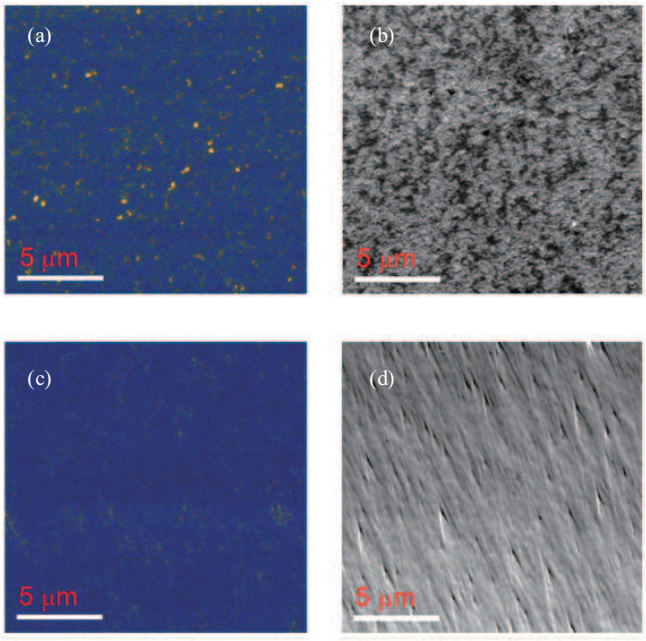


Fig. 5. (color online) Monochromatic CL images and SEM pictures recorded at 2.15 eV for polar ((a) and (b)) and semipolar plane InGaN ((c) and (d)), respectively.

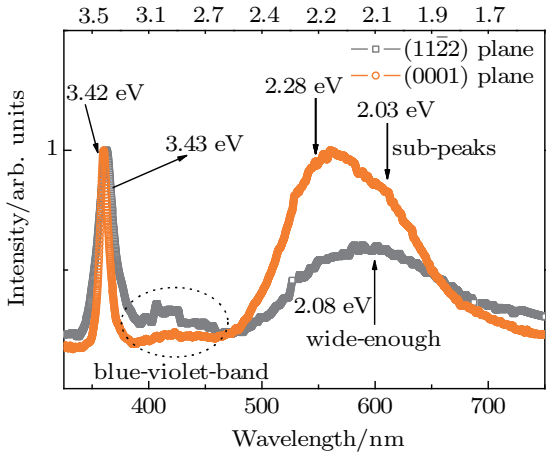


Fig. 6. (color online) Room temperature PL measurements of ($11\bar{2}2$) and (0001) surface InGaN/GaN.

The results from RSMs and PL spectrum both indicate that semipolar ($11\bar{2}2$) surface InGaN contains higher indium than polar (0001) surface. To further verify the results, SIMS (Cameca 6F) measurements are performed as shown in Fig. 7. The thickness values of the two samples are similar and the InGaN and GaN layer are about 0.1-μm and 0.85-μm thick,

respectively. During the entire InGaN growth stage, the indium incorporation of the (11$\bar{2}$2) plane is higher than that of the (0001) plane, which can be concluded that the indium intensities are 8.8×10^4 counts/sec for semipolar plane and 7.1×10^4 counts/sec for polar plane at the 70-nm depth, respectively.

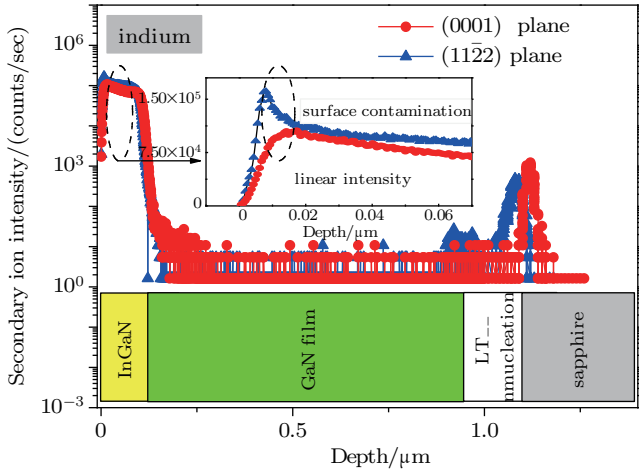


Fig. 7. (color online) SIMS results of In between (11$\bar{2}$2) and (0001) plane InGaN/GaN.

Indium incorporation is an important issue because higher incorporation is essential for LEDs with long visible wavelengths. Interestingly, the indium incorporation which has been reported was found to be distinctly different. A few theoretical studies confirmed that indium is more efficiently incorporated into InGaN grown on semipolar planes compared with on traditional polar (1$\bar{1}$00) or (0001) plane.[29,30] Durnev *et al*. demonstrated higher indium content in (11$\bar{2}$2) plane green-light InGaN LED.[31] However, Dinh *et al*. drew the completely opposite conclusion after comparing the indium content of (11$\bar{2}$2) plane InGaN layer with that of (0001) plane InGaN layer.[32,33] Furthermore, Wernicke *et al*. reported that the indium content of InGaN is also easy to affect by temperature.[34] Compared with previous experimental results, we obtain that the (11$\bar{2}$2) surface contains higher indium than the (0001) surface. Indium incorporation is known to depend on the crystallographic orientation, enhanced in (10$\bar{1}$1) plane or inhibited in (1$\bar{1}$00) plane.[35] The role of crystallographic orientation in enhancing the indium incorporation for the (11$\bar{2}$2) plane might not be negligible. However,the relevant mechanism remains to be further researched.

4. Conclusions

In this research, we successfully realize a high indium semipolar (11$\bar{2}$2) plane InGaN layer on sapphire through introducing the PMOCVD method, which is determined by HRXRD and PL simultaneously. The relevant morphology, structural and optical characteristics are also investigated. The island-like morphology for (0001) surface caused by rough-island coalescence and the spiral-like morphology for (11$\bar{2}$2) surface are both attributed to V-shape defect in variable orientations. In addition, we compare with the indium composition obtained from RSMs and find that (11$\bar{2}$2) plane has a very homogeneous indium incorporation, which is confirmed by monochromatic CL images. The PL measurements reveal that the (11$\bar{2}$2) InGaN layer emission peak wavelength is beyond 600 nm in comparison with 577 nm of (0001) InGaN layer, indicating that the (11$\bar{2}$2) surface contains higher indium content. The conclusion is further identified by the SIMS results. The PMOCVD method in the semipolar InGaN may open up possibilities for improving radiative efficiency in the long wavelength LED and LD.

References

[1] Wei T B, Hu Q, Duan R F, Wei X C, Huo Z Q, Wang J X, Zeng Y P, Wang G H and Li J M 2009 *J. Cryst. Growth* **311** 4153

[2] Xu S R, Hao Y, Zhang J C, Xue X Y, Li P X, Li J T, Lin Z Y, Liu Z Y, Ma J C, He Q and Lv L 2011 *Chin. Phys. B* **20** 107802

[3] Xu S R, Hao Y, Zhang J C, Zhou X W, Cao Y R, Ou X X, Mao W, Du D C and Wang H 2010 *Chin. Phys. B* **19** 107204

[4] Waltereit P, Brandt O, Trampert A, Grahn H T, Menniger J, Ramsteiner M, Reiche M and Ploog K H 2000 *Nature* **406** 865

[5] Xu S R, Hao Y, Zhang J C, Jiang T, Yang L A, Lu X L and Lin Z Y 2013 *Nano Lett.* **13** 365

[6] Okamoto K, Kashiwagi J, Tanaka T and Kubota M 2009 *Appl. Phys. Lett.* **94** 071105

[7] Enya Y, Yoshizumi Y, Kyono T, Akita K, Ueno M, Adachi M, Sumitomo T, Tokuyama S, Ikegami T, Katayama K and Nakamura T 2009 *Appl. Phys. Express* **2** 082101

[8] Kyono T, Yoshizumi Y, Enya Y, Adachi M, Tokuyama S, Ueno M, Katayama K and Nakamura T 2010 *Appl. Phys. Express* **3** 011003

[9] Yamamoto S, Zhao Y, Pan C C, Chung R B, Fujito K, Sonoda J, Denbaars S P and Nakamura S 2010 *Appl. Phys. Express* **3** 122102

[10] Zhao Y, Tanaka T, Yan Q, Huang C Y, Chung R B, Pan C C, Fujito K, Feezell D, Walle C G V, Speck J S, DenBaars S P and Nakamura S 2011 *Appl. Phys. Lett.* **99** 051109

[11] Zhao Y, Tanaka S, Pan C C, Fujito K, Feezell D, Speck J S, DenBaars S P and Nakamura S 2011 *Appl. Phys. Express* **4** 082104

[12] Funato M, Ueda M, Kawakami Y, Narukawa Y, Kosugi T, Takahashi M and Mukai T 2006 *Jpn. J. Appl. Phys.* **45** L659

[13] Xu S R, Zhao Y, Jiang T, Zhang J C, Li P X and Hao Y 2016 *Chin. Phys. Lett.* **33** 068102

[14] Lee S N, Kim K K, Nam O H, Kim J H and Kim H 2010 *Phys. Status Solidi B* **7** 2043

[15] Oh D S, Jong J J, Nam O, Song K M and Lee S M 2011 *J. Cryst. Growth* **326** 33

[16] Benjamin L, Wang D, Sheng K Y and Han J 2015 *Phys. Status Solidi B* **9** 13

[17] Zhang Y C, Zhou X W, Xu S R, Zhang J F, Zhang J C and HaoY 2016 *Appl. Phys. Express* **9** 061003

[18] Zhang Y C, Zhou X W, Xu S R, Wang Z Z, Zhao Y, Zhang J F, Chen D Z, Zhang J C and HaoY 2015 *Appl. Phys. Lett.* **106** 152101

[19] Ploch S, Wernicke T, Dinh D V, Pristovsek M and Kneissl M 2012 *J. Appl. Phys.* **111** 033526

[20] Neugebauer J 2001 *Phys. Status Solidi B* **227** 93

[21] Vickers M E, Kappers M J, Datta R, Mcaleese C, Smeeton T M and Rayment F D G 2005 *J. Phys. D: Appl. Phys.* **38** 99

[22] Romanov A E, Young E C, Wu F, Anurag T, Gallinat C S, Nakamura S, DenBaars S P and Speck J S 2012 *J. Appl. Phys.* **109** 103522

[23] Schuster M, Gervais P O, Jobst B, Hösler W, Averbeck R, Riechert H, Iberl A and Stömmer R 1999 *J. Phys. D: Appl. Phys.* **32** 56

[24] Pereira S, Correia M R, Pereira E, O'Donnell K P, Martin R W, White M E, Alves E, Sequeira A D and Franco N 2002 *Mater. Sci. Eng. B* **93** 163

[25] Bhat R and Guryanov G M 2015 *J. Cryst. Growth* **433** 7

[26] Selke H, Amirsawadkouhi M, Ryder P L, Böttcher T, Einfeldt S, Hommel D and Bertram F 1999 *J. Christen. Mater. Sci. Eng. B* **59** 279

[27] Damilano B and Gil B 2015 *J. Phys. D: Appl. Phys.* **48** 403001

[28] D O Demchenko, I C Diallo and M A Reshchikov 2016 *J. Appl. Phys.* **119** 035702

[29] Northrup J E 2009 *Appl. Phys. Lett.* **95** 133107

[30] Yayama T, Kangawa Y, Kakimoto K and Koukitu A 2013 *Jpn. J. Appl. Phys.* **45** 08JC02

[31] Durnev M V, Omelchenko A V, Yakovlev E V, Evstratov I Y and Karpov S Y 2011 *Phys. Status Solidi A* **208** 2671

[32] Dinh D V, Pristovsek M and Kneissl M 2015 *Phys. Status Solidi B* **8** 1

[33] Dinh D V, Oehler F, Zubialevich V Z, Kappers M J, Alam S N, Caliebe M, Scholtz F, Humphreys C J and Parbrook P J 2014 *J. Appl. Phys.* **116** 153505

[34] Wernicke T, Schade L, Netzel C, Rass J, Hoffmann V, Ploch S, Knauer A, Weyers M, Schwarz U and Kneissl M 2012 *Semicond. Sci. Technol.* **27** 024014

[35] Browne D A, Young E C, Lang J R, Hurni1C A and Speck J S 2012 *J. Vac. Sci. Technol. A* **30** 041513